Effect of Welding Condition on Solidification Structure in Weld Metal of Aluminum Alloy Sheets†

Yoshiaki ARATA*, Fukuhisa MATSUDA and Akira MATSUI*****

Abstract

Bead on plate welding was performed on 1 to 1.2 mm thick sheets of 1050 commercially pure aluminum and 3003, 5083, 6061 and 2024 clad (with 0.2 mm thick 1050) aluminum alloys with both TIG arc and electron beam weldings. Firstly, the investigation was made on optimum welding conditions of each material and the consideration was made on that result from heat conduction theory.

Secondly the relation between the welding conditions and the solidification structure in weld metal of each material was investigated. Solidification structures of the weld metal were varied largely when the welding conditions and the materials were changed. Stray crystals were developed in each material except 3003 at a low welding speed of TIG arc and at every welding speeds of electron beam. In 3003, axial crystals were developed parallel to the welding direction at a low welding speed. Equiaxed crystals were developed in every materials and the ease of development of this crystal was greatly affected by solute content, heat input and welding speed. The consideration was made on these three crystals.

1. Introduction

Many investigations have been made on the solidification mode in weld metal of aluminum and aluminum alloys and, consequently, it has been made clear that there are the stray crystal, the equiaxed crystal and the feathery crystal etc. besides columnar crystal which grew epitaxially in weld metal of aluminum and aluminum alloys. Moreover several investigations have been made on these structures crystallographically and heat conductively[1], and these investigations have been made clear their property, condition of development and factor of origination etc. However, it has not been made clear how to change the solidification structure in weld metal according to the difference of materials and the variation of welding conditions.

Therefore, in this investigation the authors aimed to make clear the effect of materials and welding conditions on solidification mode in weld metal of aluminum and aluminum alloys.

Therefore, after the bead-on-plate welding was performed on commercially pure aluminum and several aluminum alloys under various welding conditions with TIG arc and electron beam welding, the optimum welding conditions of each material were investigated experimentally and theoretically from view point of conduction theory using Wells' equation. Nextly the relation between the welding condition and the solidification structure in weld metal was investigated. Furthermore the investigation was made on condition for origination of the stray crystal, originating boundary for the equiaxed crystal and change of amount of the equiaxed crystal in weld bead.

In this investigation, thin thick sheets (1.0 mm or 1.2 mm) were used to take a two dimensional weld bead and make simple a solidification mode.

2. Materials used and Experimental procedure

Materials used in this investigation are commercial 1050 aluminum and 3003, 5083 and 6061 aluminum alloys, and 2024 aluminum alloy which was claded 0.2 mm thick 1050 aluminum on surface (in this report, this material is called 2024 clad). 1 mm thick sheets in 1050, 3003 and 5083 and 1.2 mm thick sheets in 6061 and 2024 clad were used. Specimen size was 150 mm in width and 300 mm in length. Chemical compositions of each material are tabulated in **Table 1.**

Bead on plate welding was performed by TIG arc with D. C. R. P. (4.8 mm tungsten electrode) using argon gas of 18 *l*/min as a shielding gas and by electron beam using a E. B. welder of maximum power of 6 kW (150 kV, 40 mA). In welding, a specimen was completely restrained with a restraint jig before welding. The welding speed was changed in several stages from 12.5 to 150 cm/min with TIG arc and from 150 to 350 cm/min with electron beam. Several welding heat inputs were adopted at each welding speed so that the welding might be performed to get

† Received on Dec. 26, 1973
* Professor
** Associate Professor
*** Co-operative Researcher (1973), Heavy Apparatus Engineering Laboratory, Tokyo Shibaura Electric Co., Ltd.

Table 1. Chemical Compositions of the Materials used (wt %).

Materials	t (mm)	Cu	Si	Fe	Mg	Mn	Zn	Cr	Ti	Al
1050	1.0	0.02	0.10	0.29	<0.01	<0.01	0.02	<0.01	<0.01	Bal.
2024 Clad* (Weld Metal)	1.2	4.1	0.14	0.24	1.6	0.49	<0.01	<0.01	<0.01	Bal.
3003	1.0	0.01	0.10	0.60	—	1.1	0.02	—	—	Bal.
5083	1.0	0.20	0.14	0.19	4.60	0.70	0.01	0.11	0.01	Bal.
6061	1.2	0.26	0.54	0.18	1.09	0.02	0.02	0.17	0.01	Bal.

* Chemical composition shows that of weld metal. Base metal is clad with 0.2 mm thick 1050 aluminum.

Table 2. Welding Conditions Adopted

Materials	TIG (DCRP)			EBW		
	Arc Voltage E (V)	Welding Current I (A)	Welding Speed V (cm/min)	Accelerating Voltage E (kV)	Beam Current I (mA)	Welding Speed V (cm/min)
1050	20	40～140	12.5～150	80, 120	5～16	150～350
2024 Clad	20	30～130	12.5～150	80, 120	6～16	150～350
3003	20	30～130	12.5～150	80, 120	4～16	150～350
5083	—	—	—	80, 120	3～16	150～350
6061	20	40～150	12.5～150	80, 120	6～18	150～350

a full penetrated weld bead and moreover not to get a burnt-through weld bead. Welding conditions of each material are tabulated in **Table 2.** Every weld beads were chemically etched with 6ccHF+26ccHNO_3 +78ccHCl for revealing macrostructure and solidification macrostructures were observed by means of conventional optical microscope.

3. Optimum welding conditions

3-1 Optimum welding conditions of each material used

Each material shows the respective optimum welding conditions. Experimental results are collectively shown in **Fig. 1** as optimum conditions. Optimum conditions for TIG arc are shown in left side and optimum conditions for electron beam in right side in Fig. 1. In Fig. 1, the abscissa and the ordinate represent the welding speed V (cm/min) and the heat input Q (cal/sec), respectively. The heat input Q was calculated by using Eq. (1);

$$Q = 0.24 \cdot \eta \cdot E \cdot I \quad \text{----------(1)}$$

where η: heat efficiency (the authors used the value of 0.6 at TIG arc and 0.8 at electron beam as η in this investigation), E: arc voltage for TIG arc and accelerating voltage for electron beam (V), I: welding current for TIG arc and beam current emitted for electron beam (A).

Moreover the line in the lower part in Fig. 1 shows the typical welding condition calculated to make weld bead having 1 mm wide fusion zone for 1 mm thick 5083 aluminum alloy sheet, which is leaded from

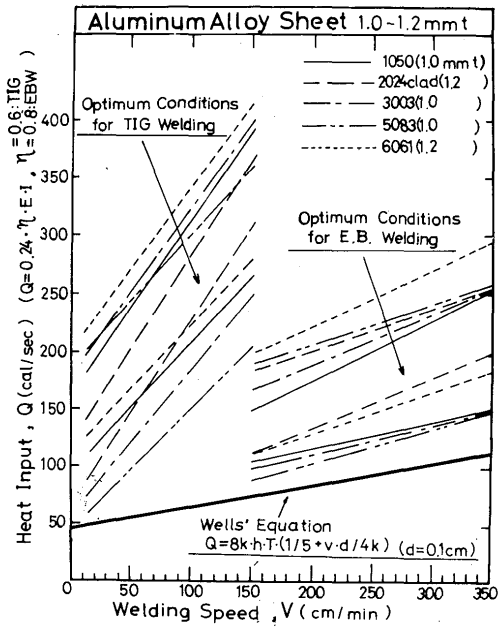

Fig. 1. Optimum welding conditions of the materials used.

Wells' equation Eq. (2)[2] that was theoretically introduced from two-dimensional line heat source.

$$Q = 8k \cdot h \cdot T \cdot (1/5 + v \cdot d/4k) \quad \text{----------(2)}$$

where Q: heat input (cal/sec), v: welding speed (cm /sec), h: thickness of sheet (cm), d: width of weld bead (cm), $k (= \lambda / c\rho)$: thermal diffusivity (cm^2/sec), λ: thermal conductivity (cal/sec·cm·°C), c: specific heat (cal/g·°C), ρ: density (g/cm^3), T: melting point (°C).

3-2 Discussion on optimum welding condition

Wells defined the ratio of heat input q (=Q/h) to vdρCT by the heat dissipation M value. Where heat input q is heat which is projected into unit length in welding and vdρCT is the heat which would be supplied simply to melt the width d of plate at the speed v without other losses:
i. e. M value is represented Eq. (3):

$$M = q/vd\rho CT \quad \text{----------(3)}$$

Wells calculated M value theoretically and led simple approximate equation in area of $0.1 < vd/4k < \infty$. It is Eq. (4):

$$M = 2\left(\frac{1}{5(vd/4k)} + 1\right) \quad (vd/4k = 0.1 \sim \infty) \text{----------(4)}$$

M value with each weld bead which was obtained in this experiment was calculated and, consequently, the experimental relation between M value and vd/4k was shown in **Fig. 2.** The relation between M value and vd/4k was classified by welding procedures and materials, and the experimental equations are given by

$$M = 5.2\left(\frac{1}{5(vd/4k)} + 1\right) \quad \text{----------(5)}$$

(2024 clad and 6061 with TIG arc)

$$M = 4.5\left(\frac{1}{5(vd/4k)} + 1\right) \quad \text{----------(6)}$$

(5083 with electron beam)

$$M = 3.8\left(\frac{1}{5(vd/4k)} + 1\right) \quad \text{----------(7)}$$

(1050 and 3003 with TIG arc)

$$M = 3.0\left(\frac{1}{5(vd/4k)} + 1\right) \quad \text{----------(8)}$$

(1050, 3003, 6061 and 2024 clad with electron beam)

M values which were obtained experimentally in this investigation were larger than the M value which was theoritically led by Wells. The experimental M value goes near to the theoritical M value more in thin sheet than in thick sheet for TIG arc, and as well more with electron beam than with TIG arc. It means that the melting efficiency in thin sheet and with electron beam is better than that in thick sheet and with TIG arc. The reason that M value for 5083 in electron beam is higher than that for other materials cannot be describe here. It may be due to evaporation of Mg during electron beam welding.

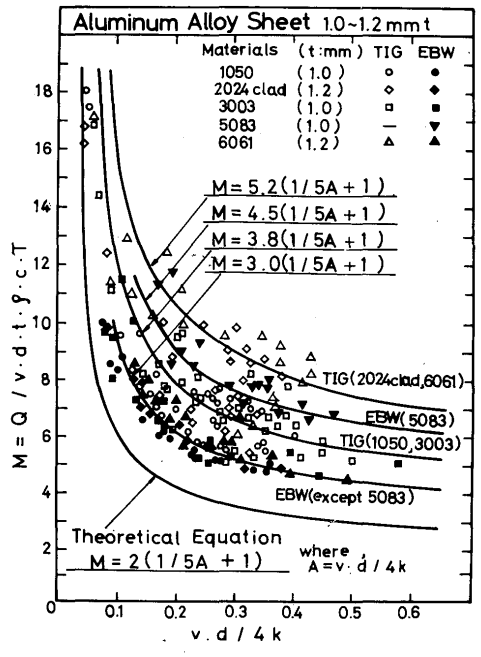

Fig. 2. Heat dissipation M value for materials used.

4. Solidification structure in weld metal

4-1 Change of solidification structures in weld metal according to variation of welding conditions

The general solidification mode in the weld metal of aluminum and aluminum alloys is schematically represented in **Fig. 3.** In Fig. 3, the distance y was directly varied between 0 % (fusion boundary) and 100 % (weld center). It has been said that there are three typical types of solidification structures in the weld metal of aluminum and aluminum alloys as shown in Fig. 3 (a). The first is the columnar crystal

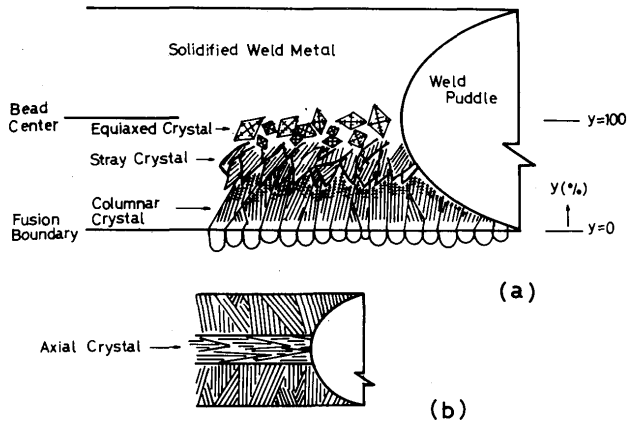

Fig. 3. General solidification structure in weld metal.

which grow epitaxially from fusion boundary, and the second is the stray crystal which is developed at the position interior of the weld metal, and the last is the equiaxed crystal which is developed at near the center of the weld metal. However, in some case, it is observed the particular solidification structure which is developed parallel to the welding direction at near the center of the weld metal as shown in Fig. 3 (b). The authors named this solidification structure the axial crystal with reference to A. V. Pectrov's[3] report. Typical macrostructures in weld metal on aluminum and aluminum alloys as mentioned above is shown in **Photo. 1.**

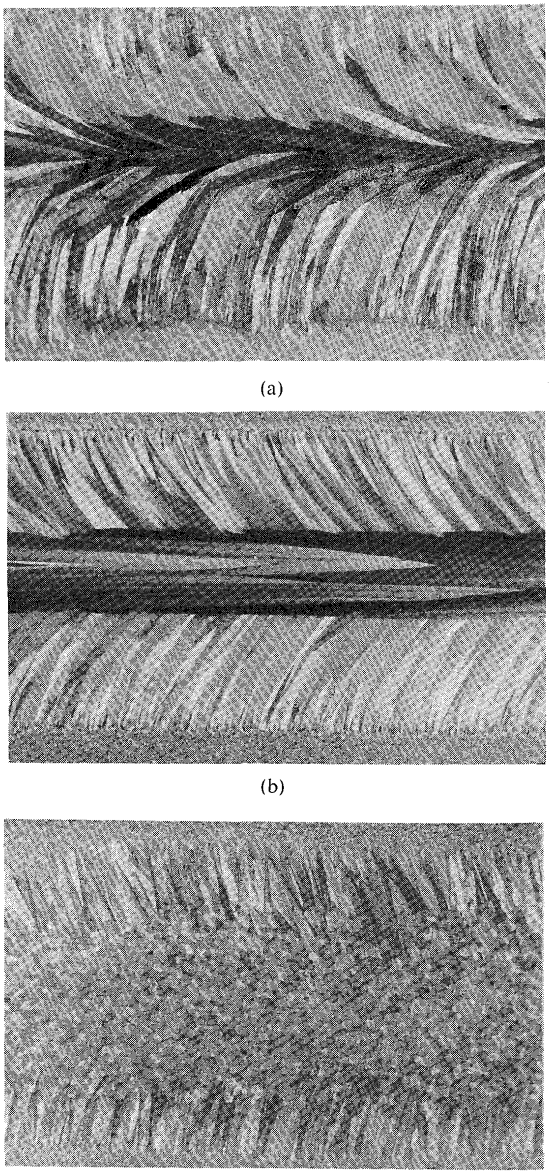

Photo. 1. Macrostructures in weld bead of aluminum alloys.
(a) Stray crystal in 1050 weld metal with TIG arc welding (V=30 cm/min, E=20 V, I=50 A)
(b) Axial crystal in 3003 weld metal with TIG arc welding (V=12.5 cm/min, E=20 V, I=40 A)
(c) Equiaxed crystal in 5083 weld metal with TIG arc welding (V=100 cm/min, E=20 V, I=100 A)

Photo. 1 (a): The stray crystal which was developed in the weld metal for low welding speed of 1050 aluminum.

(b): The axial crystal which was developed in the weld metal for low welding speed of 3003 aluminum alloy.

(c): The equiaxed crystal which was developed in the weld metal for high welding speed of 5083 aluminum alloy.

The experimental relation between the welding conditions and the solidification structure in the weld metal of each material used is described as follows;

(1) 1050 Aluminum sheet

The change of solidification structures in the weld metal of 1050 aluminum sheet according to the variation of welding conditions is shown in **Fig. 4.** The abscissa and the ordinate represent the welding speed and the heat input, respectively. Symbols of white spot and black spot represent the complete columnar crystal bead and the partial equiaxed crystal bead, respectively, and y=50, 60 % and so on represent the originating location for the stray crystal and the equiaxed crystal in the weld metal.

As seen from Fig. 4, in weld bead of low welding speed as 12.5 cm/min for TIG arc welding, columnar crystals which grew epitaxially from fusion boundary disappeared at early position on the way of development (neighboring y=50 %) and stray crystals originated instead of them. As the welding speed increased, the originating location for stray crystals went interior and at welding speed of 90~110 cm/min stray crystals were observed quite seldom. It is due

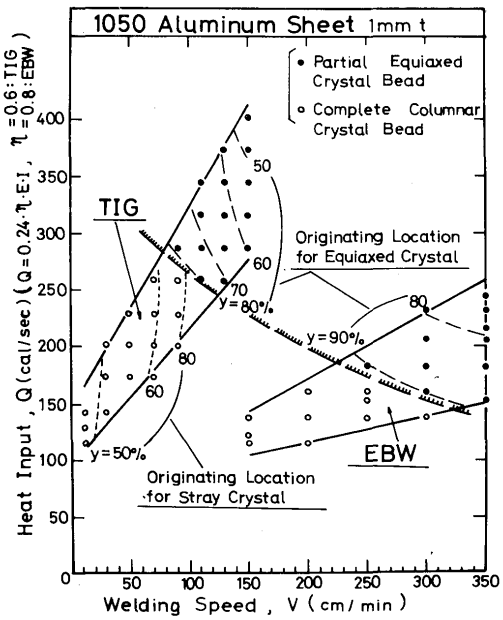

Fig. 4. Fig. 4. Change of solidification structure in 1050 aluminum sheet.

to shape of weld puddle, because increasing welding speed the shape of weld puddle changes from elliptical shaped puddle to teardrop shaped puddle. In case of teardrop shaped puddle the origination of stray crystal is not needed because the growing direction of original columnar crystal does not change as inwards growth proceeded.[4] Moreover at faster welding speed than 90 cm/min equiaxed crystals originated at near the center of weld bead. Then, the higher the welding speed, the more exterior the originating location for equiaxed crystals, that is, more wide the width which covered with equiaxed crystals in the weld bead.

On the other hand, in electron beam welding, the development of stray crystals was observed at every welding speeds and in particular at welding speed of 150～200 cm/min, columnar crystals from fusion boundary disappeared immediately after their growth and stray crystals originated and in consequent a large part of weld beads was covered by stray crystals. This is well understood from the shape of puddle in electron beam welding because low weld heat input in electron beam welding makes the puddle small and elliptical although welding speed is high enough. At faster welding speeds as 250 cm/min, the development of equiaxed crystals mixed with stray crystals began to be observed.

The broken line with hatched area shows the limit of origination of the equiaxed crystal independently of welding method.

(2) 6061 aluminum alloy sheet

The change of solidification structures in the weld metal of 6061 aluminum alloy sheet according to the variation of welding conditions is shown in **Fig. 5.** It is different a little from that in 1050. As seen from Fig. 5, in TIG arc welding the development of stray crystals was observed at welding speeds of 12.5～50 cm/min but it was not observed at welding speeds faster than 70 cm/min, and in electron beam welding it was observed at every welding speeds. On the other hand, the development of equiaxed crystals was far easier than in 1050 both in TIG arc and electron beam. That is, it was observed even at welding speed of 30 cm/min in TIG arc and 150 cm/min in electron beam. Moreover, both the higher the welding speed and the larger the heat input, the more wide the area of weld bead which was covered with equiaxed crystals.

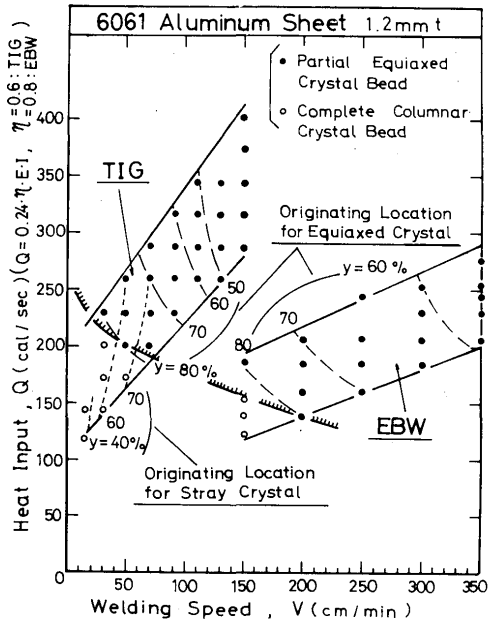

Fig. 5. Change of solidification structure in 6061 aluminum sheet.

(3) 2024 aluminum alloy clad sheet

The change of solidification structures in the weld metal of 2024 aluminum alloy clad sheet according to the variation of welding conditions is shown in **Fig. 6.** The change of solidification structures in 2024 clad was very resembled that in 6061. As seen from Fig. 6, stray crystals were developed at welding speeds of 12.5～70 cm/min in TIG arc welding and at every welding speeds in electron beam welding. Moreover, equiaxed crystals originated at welding speed of 70 cm/min in TIG arc and 200 cm/min in electron beam.

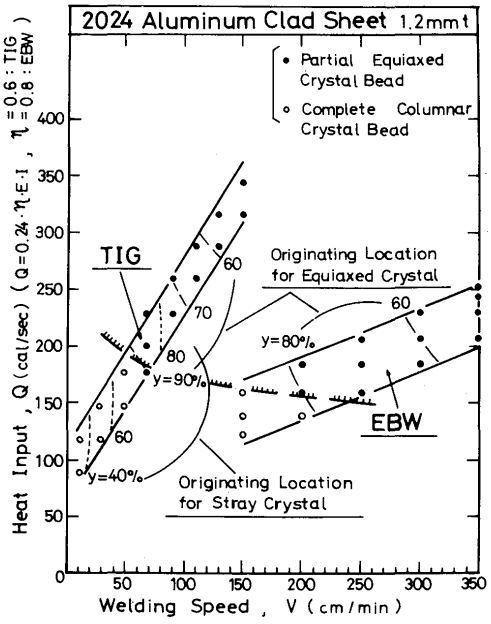

Fig. 6. Change of solidification structure in 2024 clad aluminum sheet.

(4) 5083 aluminum alloy sheet

The change of solidification structures in the weld metal of 5083 aluminum alloy sheet according to the variation of welding conditions is shown in **Fig. 7.** The authors quoted the results[5] which were obtained by Katoh et al with respect to TIG arc welding in

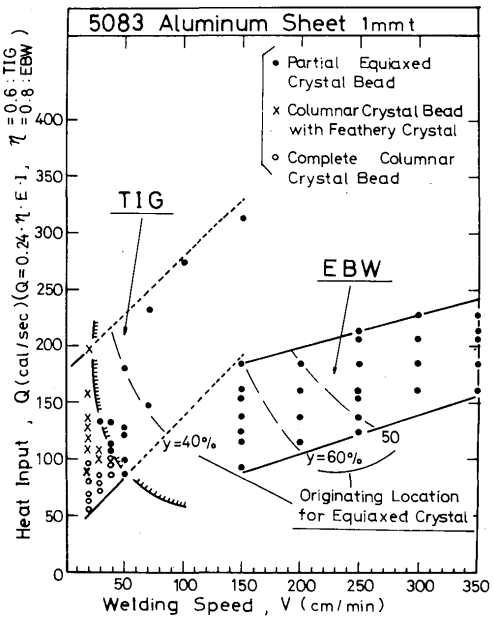

Fig. 7. Change of solidification structure in 5083 aluminum sheet.

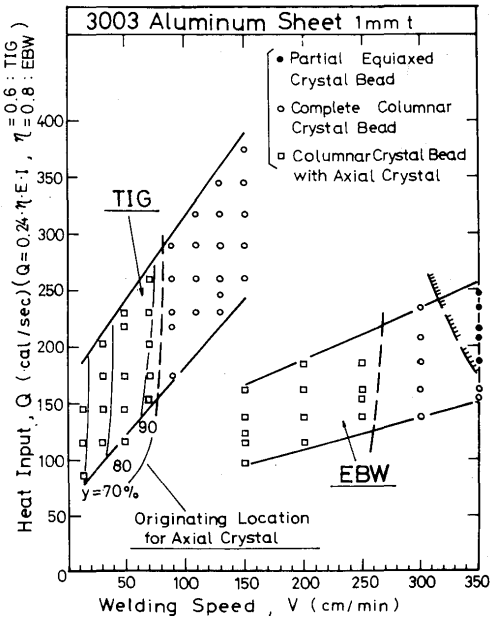

Fig. 8. Change of solidification structure in 3003 aluminum sheet.

Fig. 7. The characteristics in the weld solidification mode in 5083 aluminum alloy were the development of unique crystals, i. e. feathery crystals and easiness the development of equiaxed crystals. As shown in Fig. 7, it was reported in the former that feathery crystals were developed at low welding speeds of 12.5 ~30 cm/min in TIG arc welding. (Symbols of cross represent the feathery crystal)

The development of equiaxed crystal in 5083 was the easiest in all materials used. In TIG arc welding, many equiaxed crystals originated even at a low welding speed of 30 cm/min and in electron beam welding, equiaxed crystals were developed at every welding speeds. Moreover, the width which was covered with equiaxed crystals in weld beads of 5083 was the most wide in all materials used.

(5) 3003 aluminum alloy sheet

The change of solidification structures in the weld metal of 3003 aluminum alloy sheet according to the variation of welding conditions is shown in **Fig. 8.** As seen from Fig. 8, unique solidification mode was observed in 3003 alloy. That is the development of new crystal named the axial crystal. The columnar crystal bead with axial crystal is represented by symbols of square and originating location for axial crystalsis represented by y=70, 80 and 90 %.

In 3003, in TIG arc welding, the development of stray crystals was quite seldom and the development of equiaxed crystals were not al all but instead of their crystals the development of axial crystals which were parallel to the welding direction were observed at near the center of the weld metal at low welding speeds of 12.5 ~70 cm/min. The width which was covered with axial crystals in weld bead become narrow and narrower as the welding speed increased and the development of axial crystals were not observed at a welding speed faster than 90 cm/min as shown in Fig. 8.

Moreover, the similar tendency was observed in electron beam welding. The development of axial crystals was observed at welding speeds of 150 ~250 cm/min and it was not observed at welding speeds faster than 300 cm/min. At a welding speed of 350 cm/min and moreover at heat input larger than 180 cal/sec, equiaxed crystals originated for the first time.

4-2 Condition for origination of stray and axial crystals

Katoh et al.[6] investigated on the origination of the stray crystal crystallographically and made clear as follows:

Stray crystals originates when the direction of the maximum temperature gradient at the solid-liquid interface of a columnar crystal which has been growing from the fusion boundary has deviated from the nearest <100> direction by 40 to 50°.

As mentioned above, in this investigation it was also observed that stray crystals were developed in 1050, 2024 clad and 6061 and axial crystals were developed in 3003 instead of stray crystals. The investigation was made on the origination of the stray and the axial crystal by examinating of the relation between the direction of the maximum temperature gradient and the growth direction of the crystal.

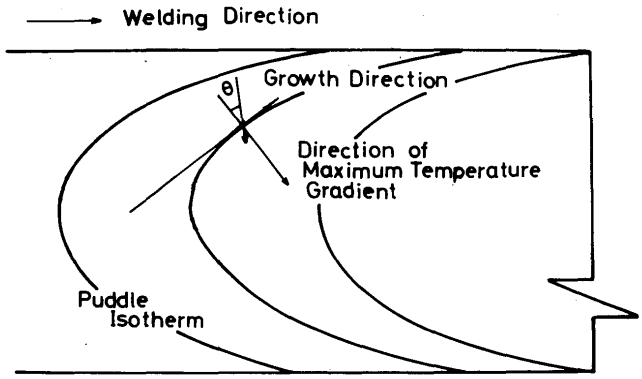

Fig. 9. Schematic representation of θ which is the angle between the growth direction of columnar crystal from fusion boundary and the direction of the maximum temperature gradient.

As shown in **Fig. 9,** θ which is the angle between the growth direction of columnar crystal from fusion boundary and the direction of the maximum temperature gradient when the stray or the axial crystal began to be developed was measured in weld metal of each material used, and, consequently, the result as shown in **Fig. 10** was obtained.

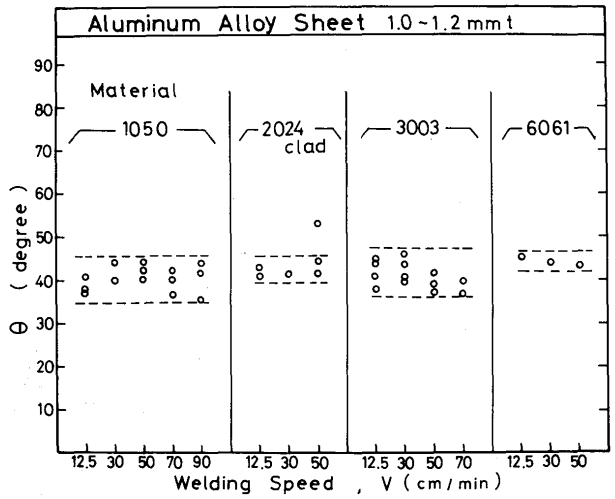

Fig. 10. Variation of angle θ in each material.

The typical example of microstructures when stray crystals originated is shown in **Photo. 2.** The relation between the growth direction of columnar crystal and the weld ripple when stray crystals originated is shown clearly in Photo. 2.

As seen from Fig. 10, it became clear that there was the rule in regard to the origination for stray or axial crystals without relating materials and welding variables. That is, stray or axial crystals originated when the growth direction of columnar crystals from fusion boundary deviated from the direction of the maximum temperature gradient, that is, vertical to puddle isotherm, by 35 to 45°. From these results it is thought that the development of stray crystals was

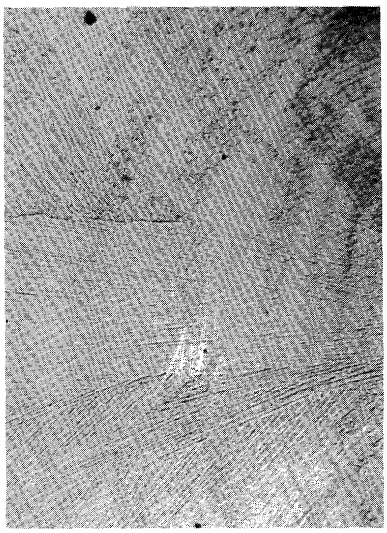

Photo. 2. An example of stray crystal which originated in the weld metal of 1050 aluminum (×42)

affected greatly by the shape of the weld ripple. This thought proved the cause why stray crystals were developed mainly at low welding speed in TIG arc and at all welding speeds in electron beam, the weld puddle of which usually showed elliptical shape. Considering from the method of their development, it is also thought that the axial crystal which was observed only in 3003 is a very resembled crystal to the stray crystal and is a kind of varied type of the stray crystal and moreover is a crystal the easy growth direction of which is agreeded with the welding direction.

4-3 Origination for equiaxed crystal

The limit lines from which the equiaxed crystal was originated according to welding conditions were shown individually with each material used in Fig. 4 through 8 in 4-1. They were rewritten collectively in **Fig. 11.** As shown Fig. 11, the case of the development of equiaxed crystals was arranged in a order 5083, 6061, 2024 clad, 1050 and 3003. It means that the development of the equiaxed crystals is depended greatly on the solute content of materials. From this thought, the investigation was made on the extent of constitutional supercooling zone. The extent of constitutional supercooling zone, X, when equiaxed crystals originated was roughly estimated Eq. (9)[5]

$$X \fallingdotseq \Delta T/G \quad \text{---------- (9)}$$

where ΔT: the temperature difference between nominal liquidus and solidus points of materials used (°C), G: the temperature gradient at melting point (°C/cm) which is theoretically given by Eq. (10)

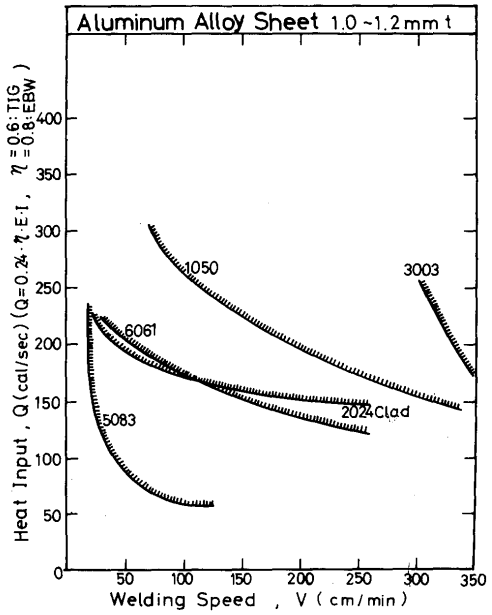

Fig. 11. Collective representation of originating location for equiaxed crystal.

$$G = 2\pi\lambda c\rho(h/Q)^2 \cdot V \cdot (T_m - T_0)^3 \quad \text{----------(10)}$$

where, T_m is assigned at the middle temperature between liquidus and solidus and T_0 is the initial temperature of sheet (°C). Now it was calculated by Eq. (9) the extent of the consititutional supercooling zone for each material at Q: 200 cal/sec, as V: the critical welding speed for origination of equiaxed crystal in each material and T_0: 0°C. The results obtained for each material used were shown in **Table 3.** The absolute values in regards of the extent of the constitutional supercooling zone, X, in the Table 3 are not reliable and it would be responsible in the value of G. Actual G value during solidification would be higher than the calculated G. However, it is understood that the origination of equiaxed crystal is strongly depended on the extent of constitutional supercooling zone, X, and the solidification temperature range, ΔT, which is related to the maximum supercooling temperature. Moreover, to be explained the origination of equiaxed crystal the authors think that it must be taken into consideration the flow mechanism of molten metal during welding in addition to the constitutional supercooling.

Table 3. Extent of Constitutional Supercooling Zone When Equiaxed Crystals Originate (at Q=200 cal/sec).

Materials	T_L(°C)	T_S(°C)	ΔT (°C)	X (mm)
1050	657	643	14	0.29
2024 Clad*	638	502	136	17.0
3003	654	643	11	0.17
5083	638	574	66	26.7
6061	652	582	70	6.2

* The values of T_L, T_S and ΔT is quoted from 2024 aluminum alloy.

5. Conclusion

Investigation have been made on optimum welding conditions and on effect of welding conditions on solidification mode in weld metal of aluminum and aluminum alloys. Main conclusions obtained are as follows:

(1) The difference of optimum welding conditions accroding to each meterial is not large so much as far as the same welding method. However the difference of the optimum welding conditions is considerable between TIG arc and electron beam welding.

(2) M values which were obtained in this experiment go near to the theoretical M value more in thin sheet than thick sheet, and as well more in electron beam than TIG arc.

(3) The solidification structure in the weld metal varies largely according to the difference of materials.

(4) The development of stray crystals is affected greatly by the shape of the weld puddle. So that, stray crystals are developed mainly at low welding speed in TIG arc and are developed at every welding speed in electron beam welding.

(5) Stray crystal originates when the growth direction of columnar crystals from fusion boundary has deviated from the direction of the maximum temperature gradient by 35 to 45°.

(6) Axial crystal which was observed only in 3003 is a kind of varied type of stray crystal and plays a part of stray crystal.

(7) The development of equiaxed crystal is affected greatly by the solute content of materials. Then, in same material, it becomes easy for equiaxed crystal to develop as both welding speed and heat input are increased.

Acknowledgement

The authors wish to thank Mr. Hiroji Nakagawa, graduate student of the welding department of the Faculty of Engineering, for his successive co-operation, and also Mr. Toshiyasu Fukui, senior researcher, Sumitomo Light Metals Co., for his advice.

References

1) H. Nakagawa, M. Katoh, F. Matsuda and T. Senda: "X-ray Investigation on Solidification Structures in Weld Metal", Trans. JWS, Vol. 1 (1970) pp94.
2) A. A. Wells: "Heat Flow in Welding", Welding J., 31 (1952) 263-S.
3) A. V. Petrov and V. I. Birman: "Solidification of Weld Metal in Pulsed Arc Welding", Autom. Welding., (1968) No. 6 ppl.
4) M. Katoh, F. Matsuda and T. Senda: "Solidification Mode in Aluminum Weld Metal", Trans. JWS, Vol. 3 (1972) pp69.
5) H. Nakagawa, M. Katoh, F. Matsuda and T. Senda: "Formation Mechanism and Metallurgical Properties of the Feathery Crystal in Weld Metal of 5083 Aluminum Alloy Sheet", Trans. JWS, Vol. 3 (1972) pp54.
6) H. Nakagawa, M. Katoh, F. Matsuda and T. Senda, "Crystallographic Investigation for Origination of New Columnar Crystal in Aluminum Weld Metal Using Single Crystal Sheet", Trans. JWS, Vol. 2 (1971) ppl.